

## $\alpha$ -decay spectroscopy of light odd-odd Bi isotopes - II: $^{186}\text{Bi}$ and the new nuclide $^{184}\text{Bi}$

A.N. Andreyev<sup>1,a</sup>, D. Ackermann<sup>2,5</sup>, F.P. Heßberger<sup>2</sup>, S. Hofmann<sup>2</sup>, M. Huyse<sup>3</sup>, I. Kojouharov<sup>2</sup>, B. Kindler<sup>2</sup>, B. Lommel<sup>2</sup>, G. Münzenberg<sup>2,5</sup>, R.D. Page<sup>1</sup>, K. Van de Vel<sup>3</sup>, P. Van Duppen<sup>3</sup>, and K. Heyde<sup>4,b</sup>

<sup>1</sup> Department of Physics, Oliver Lodge Laboratory, University of Liverpool, Liverpool L69 7ZE, UK

<sup>2</sup> Gesellschaft für Schwerionenforschung, Planckstrasse 1, D-64291 Darmstadt, Germany

<sup>3</sup> Instituut voor Kern- en Stralingsfysica, University of Leuven, Celestijnenlaan 200 D, B-3001 Leuven, Belgium

<sup>4</sup> Vakgroep Subatomaire en Stralingsfysica, University of Gent, B-9000 Gent, Belgium

<sup>5</sup> Institut für Physik, Johannes Gutenberg-University, Staudingerweg 7, D-55099 Mainz, Germany

Received: 14 March 2003 / Revised version: 29 April 2003 /

Published online: 2 September 2003 – © Società Italiana di Fisica / Springer-Verlag 2003

Communicated by J. Äystö

**Abstract.** Alpha-decay of the new nuclide  $^{184}\text{Bi}$  has been studied in the complete-fusion reaction  $^{93}\text{Nb}(^{94}\text{Mo}, 3n)^{184}\text{Bi}$  at the velocity filter SHIP. The evaporation residues were separated in-flight and subsequently identified on the basis of recoil- $\alpha$ , recoil- $\alpha$ - $\gamma$  analysis and excitation functions measurements. Two  $\alpha$ -decaying isomeric states in  $^{184}\text{Bi}$  with half-life values of 13(2) ms and 6.6(1.5) ms were identified. The  $\alpha$ -branching ratio of  $^{180}\text{Tl}$  was deduced for the first time as  $b_\alpha = (2-12)\%$ . Improved data on the fine-structure  $\alpha$ -decay of  $^{186}\text{Bi}$  were obtained in the  $^{93}\text{Nb}(^{95}\text{Mo}, 2n)^{186}\text{Bi}$  reaction. A similarity of the decay energies and half-life values of  $^{184,186}\text{Bi}$  is pointed out and a possible explanation for this effect is suggested.

**PACS.** 23.60.+e  $\alpha$  decay – 27.70.+q  $150 \leq A \leq 189$  – 27.80.+w  $190 \leq A \leq 219$

In our previous work [1] we presented the results on a detailed fine-structure  $\alpha$ -decay study of the neutron-deficient odd-odd isotopes  $^{188,190}\text{Bi}$  and on excited states in their corresponding daughter nuclei  $^{184,186}\text{Tl}$ . Similar to the heavier odd-odd mass Bi and Tl nuclei (see, for example [2] and references therein), it was shown in [1] that the residual proton-neutron interaction leads to a variety of low-lying configurations, which results in complex spectra and decay schemes of these isotopes. With the aim of extending these investigations to odd-odd Bi isotopes beyond the neutron mid-shell at  $N = 104$ , in this companion work we report on the identification of the new nucleus  $^{184}\text{Bi}$  and on the improved  $\alpha$ -decay studies of the isotope  $^{186}\text{Bi}$ .

### 1 Experimental set-up

The experimental set-up and detection system used in the present work were very similar to our previous experiments to study the nuclei  $^{188,190}\text{Bi}$ , and we refer the reader to ref. [1] for a detailed description.

<sup>a</sup> e-mail: [aan@ns.ph.liv.ac.uk](mailto:aan@ns.ph.liv.ac.uk)

<sup>b</sup> Present address: EP-ISOLDE, CERN, CH-1211, Geneva 23, Switzerland.

To produce the nuclei of interest the complete fusion reactions of  $^{94,95}\text{Mo}$  ions with the  $^{93}\text{Nb}$  target nuclei were used. Pulsed beams (5 ms on/15 ms off) of  $^{94,95}\text{Mo}$  (made from natural molybdenum) with typical beam intensities of about 10 pA on target were provided by the UNILAC heavy-ion accelerator of the GSI (Darmstadt, Germany). Eight rolled metallic  $^{93}\text{Nb}$  targets with a thickness of  $900(50) \mu\text{g}/\text{cm}^2$  were mounted on a target wheel, rotating synchronously with the UNILAC macro-pulsing. The measurements were performed at a few beam energies in the range 380–480 MeV to allow excitation functions to be determined.

After separation by the velocity filter SHIP [3–5], the evaporation residues (EVRs) were implanted into a  $300 \mu\text{m}$  thick,  $35 \times 80 \text{mm}^2$  16-strip position-sensitive silicon detector (PSSD), where their subsequent  $\alpha$ -decays were measured. Energy calibration of the PSSD was performed by using abundantly produced  $\alpha$ -decays of  $5114.9(14) \text{keV}$  ( $^{208}\text{Po}$ ),  $5304.38(7) \text{keV}$  ( $^{210}\text{Po}$ ) [6] and decays of  $6332(10) \text{keV}$  ( $^{186}\text{Pb}$ , [7]) and of  $6626(6) \text{keV}$  ( $^{184}\text{Pb}$ , [8]). The first two activities are the long-lived  $\alpha$ -decaying daughter products of heavier At, Rn and Fr nuclei, implanted in the detector in an earlier measurement. Instead of a Clover Ge detector used in [1], a single coaxial HPGe detector was installed behind the PSSD for

the  $\alpha$ - $\gamma$ /X-ray ( $\Delta T(\alpha\text{-}\gamma) \leq 5 \mu\text{s}$ ) coincidence measurements. Singles data (EVRs or  $\alpha$ -decay) or coincidence data (EVRs/ $\alpha$ - $\gamma$ ) were collected during the experiment.

## 2 Experimental results

### 2.1 $\alpha$ -decay of $^{186}\text{Bi}$

The first study of  $^{186}\text{Bi}$  was undertaken by Schneider *et al.* [9] at the velocity filter SHIP and a single  $\alpha$ -decay with  $E_\alpha = 7191(25)$  keV and  $T_{1/2} = 10(4)$  ms was assigned to this nucleus. A later study by Batchelder *et al.* [10] distinguished two  $\alpha$ -decaying isomeric states. The first had an  $\alpha$ -decay energy of  $E_\alpha = 7158(20)$  keV and a half-life of  $T_{1/2} = 15.0(17)$  ms (tentatively assigned as a  $3^+$  state), while the second, with  $E_\alpha = 7261(20)$  keV,  $T_{1/2} = 9.8(13)$  ms, was tentatively assigned as a  $10^-$  state. In both studies [9,10] only a few tens of counts were obtained.

In our experiment we collected a total number of  $^{186}\text{Bi}$  nuclei at least fifty times greater than in the previous studies [9,10]. This, along with the possibility of measuring the  $\alpha$ - $\gamma$  coincidences and excitation functions, allowed us to perform a more detailed study of this nucleus.

Figure 1 shows part of the  $\alpha$ -decay spectrum registered in the PSSD between the beam pulses in the reaction  $^{93}\text{Nb}(^{95}\text{Mo}, 2n)^{186}\text{Bi}$ . The spectrum was collected during 36 hours at a beam energy of  $E_{\text{lab}}(^{95}\text{Mo}) = 419$  MeV in front of the target, which corresponds to the maximum of the excitation function of  $^{186}\text{Bi}$ . The most intense peak at 6331(5) keV in the spectrum belongs to  $^{186}\text{Pb}$ , produced in the p,1n-channel. The recent data on two isomeric states in  $^{185}\text{Pb}$  (p,2n-channel) were discussed in ref. [11]. Based on the measured  $\alpha$ -decay energy and half-life, the peak at 7005(10) keV (inset to fig. 1) was interpreted as the known  $\alpha$ -decay of  $^{187}\text{Bi}$  ( $T_{1/2} = 32(3)$  ms, [6,12]), produced in the  $^{93}\text{Nb}(^{95}\text{Mo}, 1n)^{187}\text{Bi}$  channel.

The observation (fig. 1) of the  $\alpha$ -decay at 7263(5) keV with the measured half-life of  $T_{1/2} = 9.8(4)$  ms confirms the previous identification of the 7261(20) keV decay of  $^{186}\text{Bi}$  in [10]. The appearance of a broad energy structure with  $E_\alpha = 7070\text{--}7230$  keV (centroid at 7152(15) keV) and  $T_{1/2} = 14.8(8)$  ms is also in agreement with the data for the 7158(20) keV decay of  $^{186}\text{Bi}$  from [10]. In the following discussion, the shorter-lived and the longer-lived isomers of  $^{186}\text{Bi}$  will be denoted by  $^{186\text{m}1}\text{Bi}$  and  $^{186\text{m}2}\text{Bi}$ , respectively. A broad energy distribution of the 7070–7230 keV peak suggests that, possibly, a few different  $\alpha$ -decays and/or  $\alpha$ -e $^-$  summing effects, similar to those discussed in [1], may contribute to this group. As will be shown below,  $^{186\text{m}2}\text{Bi}$  has quite a complex decay scheme, and we cannot fully exclude the possibility that some of the decays within the 7070–7230 keV group may even belong to the fine-structure in the decay of the second (shorter-lived) isomer in  $^{186}\text{Bi}$ . Finally, the presence of a higher-energy tail/structure above the 7263 keV peak, which extends up to about 7550 keV, also points to the  $\alpha$ -e $^-$  summing effect.

The  $\alpha$ -decay properties of  $^{182}\text{Tl}$  (the daughter product of  $^{186}\text{Bi}$  after  $\alpha$ -decay) are not well established: two different  $\alpha$ -decays at 6406(10) keV [13] and at 6.05 MeV

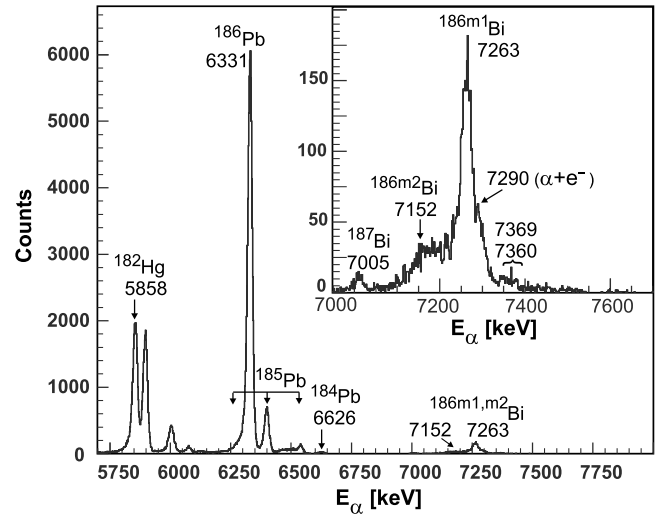


**Fig. 1.** Part of the  $\alpha$ -decay energy spectrum, collected in the PSSD between the beam pulses in the reaction  $^{93}\text{Nb}(^{95}\text{Mo}, 2n)^{186}\text{Bi}$ . Inset shows an expanded part of the spectrum for the energy region of 7000–7700 keV. Some peaks, relevant for the discussion, are labelled with the measured  $\alpha$ -decay energy (in keV) and the isotope to which the  $\alpha$ -decay belongs.

( $\alpha$ -branching ratio  $b_\alpha \leq 4\%$ ) [14] were previously reported. In [10], based on the non-observation of any  $\alpha$ -decays of  $^{182}\text{Tl}$ , a value of  $b_\alpha(^{182}\text{Tl}) \leq 5\%$  was deduced. All this makes a search for the  $\alpha_1(^{186\text{m}1,\text{m}2}\text{Bi})$ - $\alpha_2(^{182}\text{Tl})$  parent-daughter correlations quite impractical. Instead, similar to the procedure applied in [10], we searched for the  $\alpha_1$ - $\alpha_2$  events, originating from the decay sequence  $^{186\text{m}1,\text{m}2}\text{Bi} \xrightarrow{\alpha_1} ^{182}\text{Tl} \xrightarrow{\beta^+/\text{EC}} ^{182}\text{Hg} \xrightarrow{\alpha_2}$ , since  $^{182}\text{Tl}$  has a dominant  $\beta^+/\text{EC}$  decay branch to  $^{182}\text{Hg}$ . Due to much higher statistics in our case, we were able to separate the correlations starting from  $E_{\alpha_1} = 7240\text{--}7300$  keV ( $^{186\text{m}1}\text{Bi}$ ) decays and from  $E_{\alpha_1} = 7070\text{--}7230$  keV decays ( $^{186\text{m}2}\text{Bi}$ ) of  $^{186}\text{Bi}$ . In both cases ( $^{186\text{m}1}\text{Bi} \rightarrow ^{182}\text{Hg}$  and  $^{186\text{m}2}\text{Bi} \rightarrow ^{182}\text{Hg}$ ) clear correlations with the  $E_\alpha = 5858(10)$  keV decay of  $^{182}\text{Hg}$  were observed and quite similar  $\alpha$ -branching ratios of  $^{182}\text{Tl}$  could be estimated. Unfortunately, the relatively long half-lives of  $^{182}\text{Tl}$  and  $^{182}\text{Hg}$  ( $\approx 3$  s and 11 s, respectively, [6]) and a rather high counting rate in the PSSD resulted in random events in the  $\alpha_1$ - $\alpha_2$  correlation analysis, which prevented us from improving the  $\alpha$ -branching ratio of  $^{182}\text{Tl}$ . Nevertheless, it is evident that our data are in agreement with a value of  $b_\alpha(^{182}\text{Tl}) \leq 5\%$  [10].

Finally, no clear correlations with any daughter  $\alpha$ -decays of  $^{182}\text{Tl}$ , including the previously reported decays at 6406(10) keV [13] and at 6.05 MeV [14], could be observed in our data, which is also in agreement with the quoted limit for the  $\alpha$ -branching ratio of  $^{182}\text{Tl}$ .

Figure 2a shows part of the  $\alpha$ - $\gamma$  matrix ( $\Delta T(\alpha\text{-}\gamma) \leq 5 \mu\text{s}$ ), summed from the measurements at the beam energies of 419 MeV and 438 MeV. The latter energy corresponds to the maximum of the excitation function of  $^{185}\text{Bi}$ , but  $^{186}\text{Bi}$  was also produced at this energy with

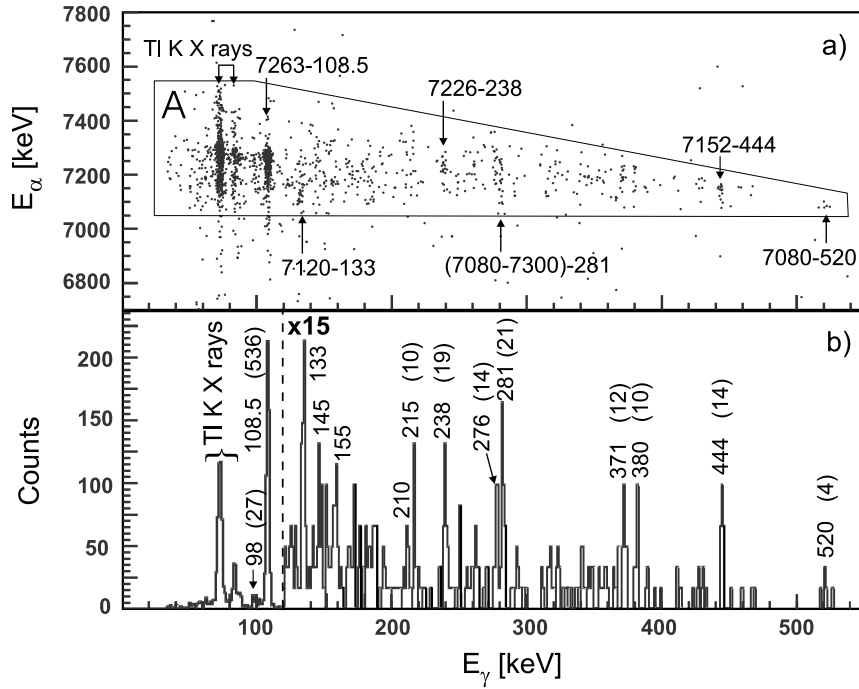


**Fig. 2.** a)  $\alpha$ - $\gamma$  matrix ( $\Delta T(\alpha\text{-}\gamma) \leq 5 \mu\text{s}$ ), summed from the measurements at beam energies of  $E(^{95}\text{Mo}) = 419$  and  $438$  MeV in front of the target. Panel b) shows the projection on the  $\gamma$  energy axis of the events from the region denoted by “A” in a). Note the different Y-scale ( $\times 15$ ) in b) starting from  $120$  keV. Some of the  $\alpha$ - $\gamma$  coincident groups and peaks relevant for discussion are marked with their  $\alpha$ -decay or/and  $\gamma$ -decay energies and the number of counts in the peak (in brackets).

a yield about 5 times lower than at  $419$  MeV. The corresponding projection on the  $\gamma$  energy axis of the events from the region, denoted by “A” in fig. 2a is shown in fig. 2b. As seen from fig. 2a,b, apart from coincidences with the Tl  $K$  X-rays, the  $7263$  keV  $\alpha$ -decay of  $^{186\text{m}1}\text{Bi}$  is also observed in strong coincidences with the  $\gamma$ -decay at  $108.5(5)$  keV (the measured half-life of this group is  $T_{1/2}(\text{recoil-[}7263\text{-}108.5 \text{ keV]}) = 9.7(7)$  ms).

As will be shown below, the Tl  $K$  X-rays in fig. 2a,b originate only partly from the conversion of the  $108.5$  keV transition, while the rest come from the conversion of a number of the low-energy ( $100$ – $500$  keV) transitions in  $^{182}\text{Tl}$ . Therefore, the standard method for deducing the conversion coefficients by comparing the number of the  $\alpha$ - $\gamma$  and  $\alpha$ -X-rays (see, for example, [1]) cannot be applied in this case. Nevertheless, a reliable multipolarity determination for the  $108.5$  keV transition can be made based on the following arguments. First of all, the  $\Delta T(\alpha\text{-}\gamma) \leq 5 \mu\text{s}$  condition, applied to produce fig. 2, requires the multipolarity of the  $108.5$  keV decay to be  $L \leq 2$ . However, the  $M1$  and  $M2$  multiplicities must be ruled out as the observed number of the Tl  $K$  X-rays in fig. 2a,b, even if fully assigned to the  $K$ -conversion of the  $108.5$  transition, is too low to be in agreement with the theoretical  $K$ -conversion coefficients of  $\alpha_K(108.5 \text{ keV}) = 5.8(M1)$  and  $36.5(M2)$  [15]. Despite the theoretical  $K$ -conversion coefficients for the  $E1$  and  $E2$  multiplicities are different by a factor of two only ( $\alpha_K(108.5\text{keV}) = 0.28(E1)$  and  $0.55(E2)$ ), their distinction can be quite easily made based on their total  $L$ - or  $M$ -conversion coefficients which differ

by a factor of about 50 ( $\alpha_L(\text{tot}, 108.5 \text{ keV}) = 0.055(E1)$  and  $2.8(E2)$ ;  $\alpha_M(\text{tot}, 108.5 \text{ keV}) = 0.013(E1)$  and  $0.72(E2)$  [15]). Although we could not measure the  $L$  and  $M$  X-rays with the present set-up, such a difference should be clearly seen in the  $\alpha$ - $e^-$  summing spectra in the PSSD. Indeed, the energy of the relatively low-energy electrons, arising after the  $K$ -,  $L$ -,  $M$ -conversion of the  $108.5$  keV transition will be fully or partly (if the electron escapes from the PSSD) summed up in the  $300 \mu\text{m}$  thick PSSD with the energy of the feeding coincident  $7263$  keV  $\alpha$ -decay (see, also, examples and discussion in [1]). Depending on the conversion coefficients, quite different summing effects and energy spectra should be observed in the PSSD. For example, fig. 3 shows the results of GEANT Monte Carlo simulations [16] for the  $\alpha(7263 \text{ keV})$ - $e^-$  summing for the  $E1$  and  $E2$  assumptions on the multipolarity of the  $108.5$  keV decay and taking the  $K$ -,  $L$ - and  $M$ -conversion into account. In both cases ( $E1$  or  $E2$ ) an extra shoulder at about  $7286$  keV can be seen (stronger in the case of the assumed  $E1$  multipolarity) which results from the  $\alpha(7263 \text{ keV})$ - $e^-(23 \text{ keV})$  summing with the  $K$ -electrons ( $E_{e^-} = E_\gamma - B_e(K) = 108.5 - 85.5 = 23 \text{ keV}$ , where  $B_e(K) = 85.5 \text{ keV}$  is the  $K$ -electron binding energy in the daughter Tl nuclei [6]). Such a shoulder is also seen in the inset of fig. 1 (at  $7290(10)$  keV) and it is understood as a result of such  $\alpha$ - $e^-$  summing. A second, much weaker peak, is seen in fig. 3a at about  $7360(5)$  keV, which results from the  $\alpha(7263 \text{ keV})$ - $e^-(\approx 94 \text{ keV})$  summing with the  $L_{1-3}$  electrons ( $B_e(L_{1-3}) = (15.3\text{-}12.7) \text{ keV}$  in Tl). The  $M$ -conversion, though about 4 times weaker, also adds

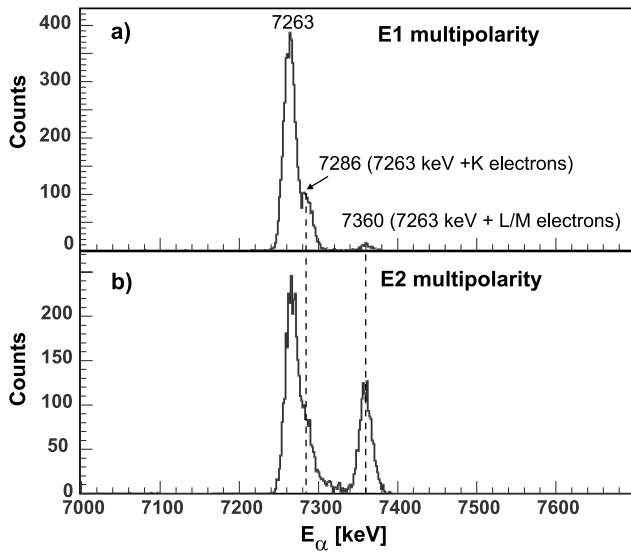


**Fig. 3.** Results of the GEANT Monte Carlo simulations for the  $\alpha(7263 \text{ keV})-e^-$  summing effects assuming either a)  $E1$  multipolarity or b)  $E2$  multipolarity for the 108.5 keV transition. Summing with the  $K$ -,  $L$ - and  $M$ -conversion electron was considered. See details in the text.

within the PSSD's energy resolution, to practically the same energy region (as  $B_e(M_{1-5}) = (3.4-2.7) \text{ keV}$ ). In contrast, assuming the  $E2$  multipolarity, the peak at 7360 keV would be about 50 times stronger (see fig. 3b), which is definitely not the case in the measured spectrum in fig. 1. On these grounds, an  $E1$  multipolarity was assigned to the 108.5 keV decay.

Based on the  $Q_{\alpha,\text{sum}} = Q_{\alpha}(7263 \text{ keV}) + E_{\gamma}(108.5 \text{ keV})$  value analysis a direct (crossover) transition with  $E_{\alpha} = 7369(5) \text{ keV}$ , which connects the  $\alpha$ -decaying state in  $^{186\text{m}1}\text{Bi}$  with the lowest state in the daughter nuclide  $^{182\text{m}1}\text{Tl}$ , should be expected for  $^{186\text{m}1}\text{Bi}$ . A weak transition with such an energy is indeed observed in fig. 1, but as seen from fig. 3a, the  $L$ - and  $M$ -conversion contributes to this region as well. The corresponding contributions were estimated in the GEANT simulations by comparing the calculated (fig. 3a) and experimental (fig. 1) intensity ratios  $I(7263)/I(7360-7369)$  of the 7263 keV and 7360–7369 keV peaks. On this basis only an upper limit of 2% for the intensity of the 7369 keV decay relative to that of the 7263 keV decay could be deduced. Therefore we consider the identification of this decay as tentative and it is shown in fig. 4 by the dashed line.

The rest of the analysis relies on the  $\alpha$ - $\gamma$  coincidence data from fig. 2a,b. As was already shown in our companion paper [1], quite complex  $\alpha$ - $\gamma$  coincidence spectra were observed in  $^{188,190}\text{Bi}$  due to the fragmentation of the  $\alpha$ -decay path to a variety of the low-lying excited multiplet states in the daughter odd-odd Tl nuclei, which result from the proton-neutron coupling (see discussion and decay schemes of  $^{188,190}\text{Bi}$  in figs. 4, 7 of [1]). In addition, the *true prompt* coincidences between the Compton-scattered  $\gamma$ -rays and the  $\alpha$ -particles, escaping from the PSSD and leaving only a part of their energy in the detector, con-

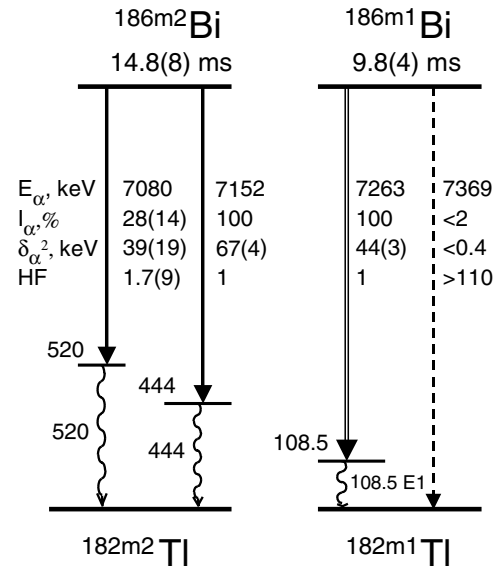


**Fig. 4.** The partial  $\alpha$ -decay schemes of  $^{186\text{m}1,2}\text{Bi}$ . Only those  $\alpha$ -decays from table 1 which could be distinguished (based on half-lives and  $Q_{\alpha,\text{sum}}$  analysis) as belonging either to  $^{186\text{m}1}\text{Bi}$  or to  $^{186\text{m}2}\text{Bi}$  are shown. The relative intensities  $I_{\alpha}$  and hindrance factors HF for the lower-intensity  $\alpha$ -decays were calculated relative to the intensity of the strongest  $\alpha$ -decay of each isomer which was normalised to  $I_{\alpha} = 100\%$  and HF = 1. The reduced  $\alpha$  widths were calculated according to [17]. The 7369 keV  $\alpha$ -decay is shown by the dashed line as tentative, see text. The relative positions of the isomers in  $^{186}\text{Bi}$  and in  $^{182}\text{Tl}$  are not known.

tribute to the continuous “background” (see discussion of figs. 3, 5 in sect. 3 of ref. [1]), which is also seen in fig. 2 of this work within the region denoted by “A”. Furthermore, the presence of the prompt low-energy partially and/or strongly converted intra- and/or inter-multiplet transitions gives rise to the  $\alpha$ - $e^-$  summing effects. In many cases this makes the exact  $E_{\alpha}$  (and, subsequently,  $Q_{\alpha,\text{sum}}$ ) value determination from the  $\alpha$ - $\gamma$  matrix quite difficult or ambiguous. All these effects were discussed in detail in [1] and we refer the reader to this paper.

Similar effects and a complex decay pattern were also observed for  $^{186}\text{Bi}$ , see fig. 2, where a number of  $\alpha$ - $\gamma$  groups with typically 10–20 events can be seen. Some of the groups in fig. 2a have well-defined  $E_{\alpha}$ -energies as, for example, the groups at 7263(5)-108.5(5) keV (discussed above), 7080(15)-520(1) keV, 7120(15)-133(1) keV, 7152(15)-444(1) keV, 7226(15)-238(1) keV. We note that a peak at 7152 keV is also present in fig. 1 and most probably represents the same decay as seen in coincidence with the 444 keV  $\gamma$ -decay.

Based on the similar value of  $Q_{\alpha,\text{sum}} = 7756(15) \text{ keV}$ , the groups at 7080(15)-520(1) keV and at 7152(10)-444(1) keV are tentatively attributed to the same isomer  $^{186\text{m}2}\text{Bi}$  (see table 1 and fig. 4). In this case a direct (crossover) 7590(10) keV  $\alpha$ -decay could be, in principle, expected for this isomer, but was not seen in our data (see inset to fig. 1).

**Table 1.** Summary of our results on  $^{184,186}\text{Bi}$ . For  $^{186}\text{Bi}$  the previous data from [10] are also shown (see text for details). Column 1 shows the final half-life of each isomer, deduced in our work, while the values for each individual decay (where deduced) are shown in column 3. Uncertainty of the  $\gamma$  energy values is 1 keV. Note that we prefer not to draw any conclusion on the spin/parity of the states in  $^{186\text{m}1, \text{m}2}\text{Bi}$ , though in [10] the longer-lived and the shorter-lived isomers were tentatively assigned the spin/parity of  $3^+$  and  $10^-$ , respectively (see discussion in the text).

Assignment, $T_{1/2}$	Our data			Reference [10]	
	$E_\alpha$ (keV)	$T_{1/2}$ (ms)	Coincident $\gamma$ 's (keV)	$E_\alpha$ (keV)	$T_{1/2}$ (ms)
$^{186\text{m}1}\text{Bi}$ , 9.8(4) ms	7263(5)	9.8(4)	108.5(5) E1	7261(20)	9.8(13)
$^{186\text{m}2}\text{Bi}$ , 14.8(8) ms	7369(10) <sup>(a)</sup>			7158(20)	15.0(17)
	7070-7230 <sup>(b)</sup>	14.8(8)	87, 98, 133, 215, 238, 276, 281, 371, 380, 444, 520		
	7080(15)		520		
	7120(15)		133		
	7152(15)		444		
$^{184\text{m}1}\text{Bi}$ , 13(2) ms	7226(15)		238		
	7120-7350 <sup>(c)</sup>	13(2)			
$^{184\text{m}2}\text{Bi}$ , 6.6(1.5) ms <sup>(d)</sup>	7194(20)	$14_{-4}^{+6}$	124		
	7220(15)	$4.6_{-1.3}^{+1.9}$	449		
	7445(35)	$8.1_{-2.2}^{+3.0}$			
	7730-7850 <sup>(e)</sup>	$6.7_{-2.2}^{+3.0}$			

<sup>(a)</sup> Tentative  $\alpha$ -decay for which only an upper limit of  $I_\alpha \leq 2\%$  was deduced.

<sup>(b)</sup> Complex structure with contributions from many  $\alpha$ -decays. The next four lines show the  $\alpha$ -decays with a well-defined  $\alpha$ -decay energy only. Due to uncertainty in the half-life determination these decays may belong to different isomers in  $^{186}\text{Bi}$ . They are shown in table separately only to provide information on the  $\alpha$ - $\gamma$  coincidence relations.

<sup>(c)</sup> Complex structure with contributions from many  $\alpha$ -decays.

<sup>(d)</sup> Based on the summed statistics for the shorter-lived  $\alpha$ -decays at 7445(35) keV, 7730-7850 keV and of for  $\alpha$ - $\gamma$  coincident events at 7220(15)-449(1) keV.

<sup>(e)</sup> Tentative  $\alpha$ -decay, see discussion in the text.

In contrast, some of the  $\alpha$ - $\gamma$  groups have a broader  $\alpha$  energy distribution due to the  $\alpha$ - $e^-$  summing as, for instance, the group at  $\alpha(7080-7300)$ - $\gamma(281(1)$  keV), or the groups in coincidence with the  $\gamma$  transitions at 371 and 380 keV.

The individual half-lives of all these groups, deduced from the recoil- $[\alpha$ - $\gamma]$  time distributions, were found to be within the interval of (8–16) ms, which supports their assignment to the decay of  $^{186\text{m}1, \text{m}2}\text{Bi}$ . However, a rather large statistical uncertainty in the half-life determination, the presence of scattered *true* prompt “escaping  $\alpha$ ”-“Compton  $\gamma$ ” “background” coincidence events (see above), and quite similar half-lives of the two isomers in  $^{186}\text{Bi}$  prohibit us from making an unambiguous assignment of these groups to a specific isomer, with the exception of the 7263-108.5 keV group.

Instead, to avoid tentative assignments, we provide only a  $\gamma$  energy projection (see fig. 2b) of the spectrum in fig. 2a. This shows the  $\gamma$  transitions occurring in coincidence with the fine-structure  $\alpha$ -decays of  $^{186}\text{Bi}$ , and proceeding between excited states in the daughter nucleus  $^{182}\text{Tl}$ . These transitions are summarised in table 1. In addition to these transitions, there are possibly some other  $\gamma$ -decays (for example, at 145(1) and 155(1) keV), but their assignment is unclear due to the low number of events. Furthermore, though a few fine-structure  $\alpha$ -decays were observed in  $^{186\text{m}1, \text{m}2}\text{Bi}$ , the direct full energy (crossover)  $\alpha$  transitions were, most probably, not observed in both

cases. The 7369(10) keV decay (see table 1) could potentially represent such a decay in  $^{186\text{m}1}\text{Bi}$ , but no solid conclusion can be drawn here as some low-energy converted transitions could have been missed in our experiment. That is why in fig. 4 we show only partial-decay schemes of two isomeric states in  $^{186}\text{Bi}$  with the  $\alpha$ -decays whose origin was established quite reliably.

We note that a proton branch of  $b_p = 85(6)\%$  was reported for  $^{185}\text{Bi}$  in ref. [18] and, therefore, the existence of a small proton branch in  $^{186}\text{Bi}$  could not be excluded. However, in our study no proton decays were observed for  $^{186}\text{Bi}$  and an upper limit for the proton branch of both isomeric states in  $^{186}\text{Bi}$  could be estimated as  $b_p \leq 0.5\%$ .

The results obtained will be further discussed in sect. 3.

## 2.2 $\alpha$ -decay of the new isotope $^{184}\text{Bi}$

The new isotope  $^{184}\text{Bi}$  was identified in the reaction  $^{93}\text{Nb}(^{94}\text{Mo}, 3n)^{184}\text{Bi}$  at several beam energies in the range of 434–461 MeV in front of the target. The main measurement ( $\approx 38$  hours) was performed at a beam energy of 444 MeV, corresponding to the maximum of the excitation function of  $^{184}\text{Bi}$ . Figure 5a shows part of the energy spectrum of  $\alpha$ -decays correlated with implants within 60 ms and registered between the beam pulses at this beam energy. The isotopes  $^{183-185}\text{Pb}$  are produced in the

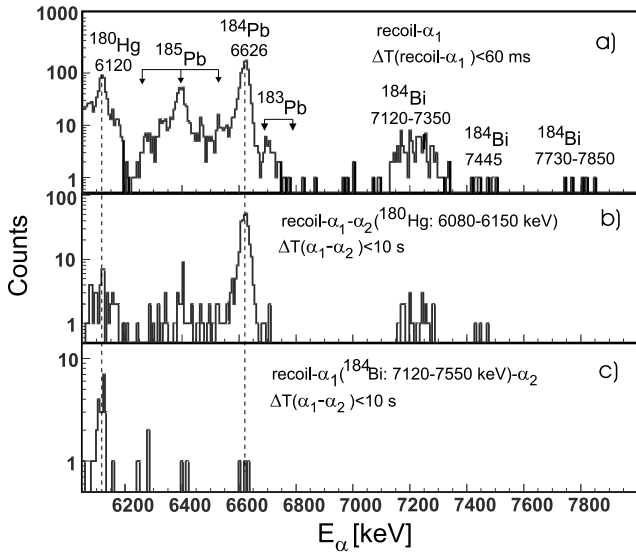


**Fig. 5.** Data obtained in the  $^{93}\text{Nb}(^{94}\text{Mo}, 3n)^{184}\text{Bi}$  reaction at  $E_{\text{lab}}(^{94}\text{Mo}) = 444$  MeV. Part a) shows  $\alpha_1$ -decays recorded in the PSSD between the beam pulses and correlated with recoils within 60 ms. Part b) has an additional condition that the recoil- $\alpha_1$  events from a) are further correlated within 10 s with the 6120 keV decay of  $^{180}\text{Hg}$ . Part c) shows the spectrum of the  $\alpha_2$ -decays from the [recoil- $\alpha_1(^{184}\text{Bi})$ ]- $\alpha_2$  analysis, with a gate on the  $E_{\alpha_1} = 7120\text{--}7550$  keV region of fig. 1a.

pxn-channel of this reaction, while a peak at 6120(5) keV represents the  $\alpha$ -decay of  $^{180}\text{Hg}$ . We also stress the cleanliness of the recoil- $\alpha_1$  correlation spectrum in the energy interval of  $E_{\alpha} = 8000\text{--}10000$  keV (not shown in fig. 5) with a sole count observed at  $E_{\alpha} = 8134$  keV and  $\Delta T(\text{recoil-}\alpha_1(8134 \text{ keV})) = 56$  ms.

The groups in fig. 5a at around 7120–7350 keV, 7445(35) keV and at 7730–7850 keV are attributed to the decay of the new isotope  $^{184}\text{Bi}$ . Below we provide the arguments for this assignment. Similar to the case of  $^{186}\text{Bi}$ , the broad energy distribution of the group at 7120–7350 keV in fig. 5a suggests that a few peaks (and possibly  $\alpha$ -e $^{-}$  summing effects) may contribute to this structure. Therefore, only a common half-life value of  $T_{1/2} = 13(2)$  ms was deduced for this peak. A half-life value of  $T_{1/2} = (8.1^{+3.0}_{-2.2})$  ms was deduced for the group at 7445(35) keV and of  $T_{1/2} = (6.7^{+3.0}_{-2.1})$  ms for the group at 7730–7850 keV. Due to somewhat different half-lives of the latter two weak groups on the one hand and of the stronger group at 7120–7350 keV on the other hand and by analogy with the heavier odd-odd mass Bi isotopes we tentatively suggest the existence of two  $\alpha$ -decaying isomeric states in  $^{184}\text{Bi}$ , one having a half-life of 6.6(1.5) ms, and the other 13(2) ms. More arguments to support this conclusion will be given later in the text.

As will be shown below, the nucleus  $^{180}\text{Tl}$  ( $T_{1/2} \approx 1.5$  s [19], the daughter product of  $^{184}\text{Bi}$  after  $\alpha$ -decay) has a relatively small  $\alpha$ -branching ratio ( $b_{\alpha} \leq 12\%$ ). Combined with its quite complex  $\alpha$ -decay scheme (at least three  $\alpha$  transitions were observed in [19]) this makes a search for recoil- $\alpha_1(^{184}\text{Bi})$ - $\alpha_2(^{180}\text{Tl})$  correlations imprac-

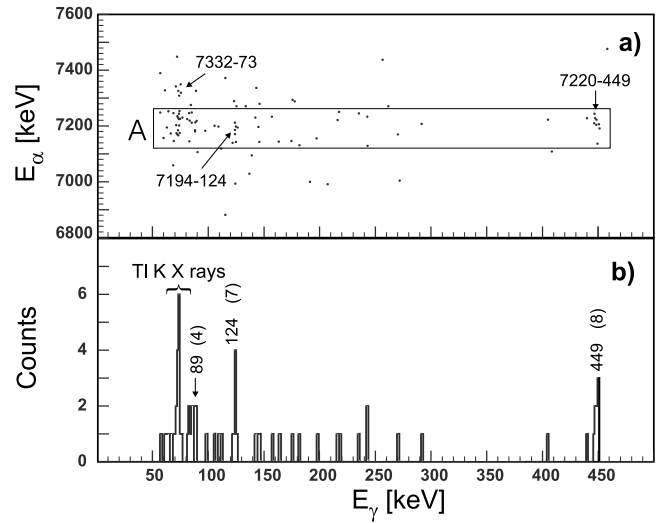


**Fig. 6.** a)  $\alpha$ - $\gamma$  matrix ( $\Delta T(\alpha\text{-}\gamma) \leq 5 \mu\text{s}$ ) collected at the beam energy  $E(^{94}\text{Mo}) = 444$  MeV in front of the target. A projection on the  $\gamma$  energy axis of the events from the rectangle “A” is shown in the panel b). The number of counts for some peaks is shown in brackets.

tical. Instead, we used the decay sequence recoil- $^{184}\text{Bi} \xrightarrow{\alpha_1} ^{180}\text{Tl} \xrightarrow{\beta^+/\text{EC}} ^{180}\text{Hg} \xrightarrow{\alpha_2}$ . Figure 5b shows the same spectrum as fig. 5a, but with the additional condition that the recoil- $\alpha_1(^{184}\text{Bi})$  pairs must further correlate within the time interval of 10 s with the  $E_{\alpha} = 6120$  keV decay of  $^{180}\text{Hg}$  ( $T_{1/2} = 2.56(2)$  s [20]). Note that, as  $b_{\alpha}(^{180}\text{Hg}) = 48(2)\%$  (see [21] and references therein) and the efficiency of the PSSD for the  $\alpha$ -particle registration is about 50%, the number of counts in fig. 5b is reduced by about a factor of 4 compared to fig. 5a. Despite this, the peaks at  $E_{\alpha_1} = 7120\text{--}7350$  keV and 7445(35) keV are present in fig. 5b, which proves that they belong to the new isotope  $^{184}\text{Bi}$ .

Due to a relatively long  $\Delta T(\alpha_1\text{-}\alpha_2)$  search interval some random correlations may occur in fig. 5b. This number can be reliably estimated based on the following arguments. The peak at 6120(10) keV in fig. 5b represents random “self-correlations” of the type [recoil- $\alpha_1(^{180}\text{Hg})$ ]- $\alpha_2(^{180}\text{Hg})$ . Therefore, by comparing the number of the 6120 keV decays in fig. 5a and fig. 5b an upper limit of 6% for the number of random correlations in fig. 5b can be obtained, which proves that the correlations at  $E_{\alpha_1} = 7120\text{--}7350$  keV and 7445 keV in fig. 5b are real. The reduced efficiency of the [recoil- $\alpha_1$ ]- $\alpha_2$  correlations (see above) may explain the absence in fig. 5b of the events at 7730–7850 keV observed in fig. 5a. Finally, as the only evidence for the group at 7730–7850 keV belonging to  $^{184}\text{Bi}$  is its high energy and the fact that its half-life is close to that of the 7445 keV group, we prefer to keep this assignment as tentative as shown in table 1.

Figure 6a shows an  $\alpha$ - $\gamma$  matrix collected at the same beam energy as fig. 5, while a projection on the  $\gamma$  energy axis from the rectangle, denoted “A” in fig. 6a, is given in fig. 6b. In addition to Tl K X-rays, the peaks at 89(1) keV (4 counts), 124(1) keV (7 counts) and at 449(1) keV (8 counts) were observed in fig. 6. Based on the limited

number of counts a half-life of  $T_{1/2} = (4.6_{-1.3}^{+1.9})$  ms was deduced for the group at 7220(15)-449(1) keV, and  $T_{1/2} = (14_{-4}^{+6})$  ms for the group at 7194(20)-124(1) keV. These values also support the conclusion that two  $\alpha$ -decaying isomeric states are present in  $^{184}\text{Bi}$  and a half-life value of 6.6(1.5) ms was deduced for the shorter-lived isomer based on the summed statistics for the shorter-lived groups at 7445(35) keV, 7730–7850 keV and for the  $\alpha$ - $\gamma$  coincident group at 7220(15)-449(1) keV. Tentatively we attribute the weak group at 7332(20)-73(1) keV (fig. 6a) to the decay of  $^{184}\text{Bi}$  as well, but the large uncertainty in its half-life determination prevents us from assigning this decay to a particular isomer in  $^{184}\text{Bi}$ .

We mention that despite the fact that a proton branch of  $b_p = 85(6)\%$  was reported for  $^{185}\text{Bi}$  in ref. [18], no proton decay could be observed in our study for  $^{184}\text{Bi}$ .

All data deduced in our study for  $^{184}\text{Bi}$  are summarised in table 1.

### 2.3 $\alpha$ -branching ratio of $^{180}\text{Tl}$

Using our data on the decay of  $^{184}\text{Bi}$  an estimate of the previously unknown  $\alpha$ -branching ratio of  $^{180}\text{Tl}$  can be made. A spectrum of  $\alpha_2$ -decays from the [recoil- $\alpha_1(^{184}\text{Bi})$ ]- $\alpha_2$  correlation analysis with a gate on the  $\alpha_1(^{184}\text{Bi}, 7120\text{--}7550\text{ keV})$  decay is shown in fig. 5c. In addition to the correlations with the decays at 6120(10) keV of  $^{180}\text{Hg}$  (see discussion above), 6 scattered events in the energy interval of 6200–6500 keV and 3 events at 6626(20) keV can be seen. The 6200–6500 keV interval potentially corresponds to the region of the  $\alpha$ -decays of  $^{180}\text{Tl}$  (at 6208(10), 6281(10), 6362(10), 6470(20) and 6560(10) keV, see [19]). The probability of random events in fig. 5c is very low as can be seen by comparing the number of the 6626 keV decays ( $^{184}\text{Pb}$ ) in fig. 5a and fig. 5c. The 3 events at 6626 keV in fig. 5c are random correlations of the type [recoil- $\alpha_1(^{184}\text{Bi})$ ]- $\alpha_2(^{184}\text{Pb})$  and therefore can be used for this purpose.

Thus, by comparing the number of the 6120 keV decays of  $^{180}\text{Hg}$  (corrected for the  $\alpha$ -branching ratio) and the number of the events at 6200–6500 keV in fig. 5c (both corrected for the possible random correlations), a value of  $b_\alpha(^{180}\text{Tl}) = 8(4)\%$  was deduced. In this estimate we neglected a possible contribution to the region of 6200–6500 keV in fig. 5c of the 6228 keV and 6286 keV decays of  $^{176}\text{Au}$  [6, 22], being the daughter of  $^{180}\text{Tl}$  after its  $\alpha$ -decay. This was done as, to our knowledge, the  $\alpha$ -branching ratio of  $^{176}\text{Au}$  is not known. In an extreme case of  $b_\alpha(^{176}\text{Au}) = 100\%$  half of the counts in the 6200–6500 keV region of fig. 5c should be attributed to  $^{176}\text{Au}$ , which would result in a value of  $b_\alpha(^{180}\text{Tl}) = 4(2)\%$ . Therefore, we give a range of (2–12)% as an estimate for the  $\alpha$ -branching ratio of  $^{180}\text{Tl}$ .

## 3 Discussion

A quite extensive general discussion of the proton-neutron multiplets in the neutron-deficient odd-odd  $^{184\text{--}196}\text{Bi}$

and their daughter Tl nuclei was given in a previous paper (sect. 4.1 and references of [1]). Therefore, in this paper only the discussion relevant for  $^{184,186}\text{Bi}$  will be emphasized, while we refer the reader to refs. [1, 2] for more general details.

### 3.1 $^{186}\text{Bi}$

In ref. [10], the spin and parity of ( $10^-$ ) and ( $3^+$ ) were tentatively assigned to the shorter-lived and longer-lived isomeric states in  $^{186}\text{Bi}$ , decaying by the 7261(20) keV and 7158(20) keV  $\alpha$ -decay, respectively. This was based on the higher intensity of the 7261 keV  $\alpha$ -decay, compared to the 7158 keV decay and taking into account that the heavy-ion complete-fusion reactions tend to populate preferentially high-spin states, which was indeed observed in the odd-odd isotopes  $^{190\text{--}194}\text{Bi}$  [2].

Furthermore, in  $^{190\text{--}196}\text{Bi}$  the reduced  $\alpha$  widths  $\delta_\alpha^2$  (calculated with the Rasmussen prescription [17]) for the  $\Delta L = 0\ 3^+ \rightarrow 3^+$  decays were always somewhat larger ( $\approx 30\text{--}60\%$ ) than the values for the unhindered  $10^- \rightarrow 10^-$  decays (see [1] and table 1 of [2]). In contrast, in  $^{188}\text{Bi}$  the  $3^+ \rightarrow 3^+$  and  $10^- \rightarrow 10^-$  decays have similar reduced  $\alpha$  widths (54(3) keV and 52(3) keV, respectively [1]) and, surprisingly, the intensity of the  $3^+ \rightarrow 3^+$  decay is somewhat *higher* than that of the  $10^- \rightarrow 10^-$  decay (see sect. 4.3.2 and fig. 1 of [1]). These facts may indicate a spin/structure change in  $^{188}\text{Bi}$  or in its daughter  $^{184}\text{Tl}$  (see sect. 4.3 of [1]). Therefore, we believe that the use of the intensity and/or reduced widths systematics alone cannot be used to provide spin/parity assignments for the lighter odd-odd Bi isotopes, starting from  $^{186}\text{Bi}$ .

Another way to shed light on the spin/parity assignments in  $^{186}\text{Bi}$  is the use of the  $\alpha$ -decay energy systematics of unhindered  $10^- \rightarrow 10^-$  and  $3^+ \rightarrow 3^+$  decays in the odd-odd  $^{188\text{--}196}\text{Bi}$  nuclei, shown in fig. 7a. This figure is an extended version of fig. 8a of [1] and includes the new data for  $^{184,186}\text{Bi}$ . In [1] we underlined the practically linear dependence of the energy of the  $10^- \rightarrow 7^+$   $\alpha$ -decays on the Bi mass number (see sect. 4.3.1 of [1]). Indeed, a linear fit of the data for  $^{188\text{--}194}\text{Bi}$  could reproduce the measured values with an error in each point close to the uncertainty of the  $\alpha$  energy measurements (see fig. 7a). Furthermore, it was shown that the energy of the  $10^- \rightarrow 10^-$   $\alpha$ -decays follows a parabolic dependence as a function of the number of valence nucleon pairs with a local maximum in  $^{192,194}\text{Bi}$  (not seen clearly due to the scale chosen for the Y-axis in fig. 7a).

As mentioned in [1] and seen from fig. 7a up to  $^{190}\text{Bi}$  the  $3^+ \rightarrow 2^-$  and  $3^+ \rightarrow 3^+$  decays behave very similarly to the  $10^- \rightarrow 7^+$  and  $10^- \rightarrow 10^-$  decays discussed above: they follow the linear and the parabolic energy dependence, respectively, on the neutron number. Moreover, the energies of the unhindered  $10^- \rightarrow 10^-$  and  $3^+ \rightarrow 3^+$  decays in  $^{190\text{--}196}\text{Bi}$  are very similar, the largest difference being only 46 keV ( $^{194}\text{Bi}$ , [2]).

Based on the above arguments we performed linear and parabolic extrapolations, respectively, of the systematics of the  $10^- \rightarrow 7^+$  and  $10^- \rightarrow 10^-$  decays for the cases



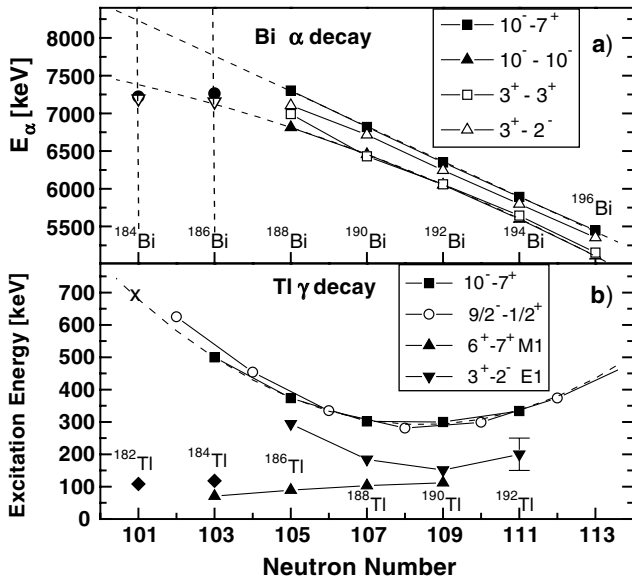


**Fig. 7.** a) Systematics of some selected  $\alpha$ -decays in the odd-odd  $^{184-196}\text{Bi}$  isotopes. Our data for  $^{184,186}\text{Bi}$  are shown by filled circles and by open down triangles. b) Systematics of the excitation energies of some selected  $\gamma$  transitions in the daughter odd-odd  $^{181-192}\text{Tl}$  isotopes and of the  $9/2^-$  intruder states in the odd-mass  $^{185-195}\text{Tl}$ . The excitation energies are given relative to the lowest state in *each particular isomer*. Extrapolations, based on the parabolic and linear fits, respectively, for the  $(10^-) \rightarrow (10^-)$  and  $(10^-) \rightarrow (7^+)$   $\alpha$ -decays in the  $^{188-196}\text{Bi}$  isotopes are shown by the dashed lines in the panel a). The same parabolic fit was used for the  $(3^+) \rightarrow (3^+)$  states (not shown in figure). The  $10^- \rightarrow 7^+$  and  $3^+ \rightarrow 2^-$   $\alpha$ -decay energies are not known in  $^{196}\text{Bi}$ , but can be deduced from fig. 2 of ref. [2]. A parabolic fit to the energies of the  $10^-$  intruder states (relative to the  $7^+$  states) in the odd-odd mass  $^{184-192}\text{Tl}$  isotopes is shown by the dashed line in the panel b). The position of the expected  $10^-$  intruder state at about 680 keV in  $^{182}\text{Tl}$  is marked by a cross. The position of the excited states at 108.5 keV in  $^{182}\text{Tl}$  and at 117.5 keV in  $^{184}\text{Tl}$  are shown by the full diamonds. Data are from this work and from refs. [1, 2, 6].

of  $^{184,186}\text{Bi}$  (dashed lines in fig. 7a). Due to the similarity of their  $\alpha$ -decay energies we used the same parabolic fit to both  $10^- \rightarrow 10^-$  and  $3^+ \rightarrow 3^+$  decays. It is clear that both the 7263 keV and 7152 keV  $\alpha$ -decays (shown in fig. 7a by full circles and by open down triangles, respectively) lie close to the extrapolated value for the  $10^- \rightarrow 10^-$  and  $3^+ \rightarrow 3^+$  decays. This situation is similar to the cases of the  $^{190-196}\text{Bi}$  nuclei, in which the energies of the  $10^- \rightarrow 10^-$  and  $3^+ \rightarrow 3^+$  decays are quite similar. The only difference between these energies was observed in  $^{188}\text{Bi}$  for the  $3^+ \rightarrow 3^+$   $\alpha$ -decay, see discussion in [1].

To summarise the experimental situation, although in the case of  $^{186}\text{Bi}$  the  $\alpha$ -decay systematics alone (intensities, reduced widths, decay energies) cannot provide the unique assignments, they suggest that the spin/parity assignments of the two observed isomers in  $^{186}\text{Bi}$  could be  $10^-$  and  $3^+$  as tentatively suggested in [10]. However, taking into account the change of the decay pattern observed in the neighbouring isotope  $^{188}\text{Bi}$ , we prefer not to draw

any conclusions or provide tentative spin/parity assignments for the two isomers in  $^{186}\text{Bi}$ .

This is also explained by the fact that, as discussed in sect. 4.1 of ref. [1], a few low-lying configurations can be expected in the lightest Bi nuclei. In particular, the  $[\pi 1h_{9/2} \times \nu 1i_{13/2}]_{2^- \rightarrow 11^-}$  configuration plays an important role with the  $10^-$  state being the lowest (isomeric) multiplet member for  $A(\text{Bi}) > 190$  nuclei (see also fig. 9 of [23]). Calculations of ref. [23] suggest that for  $A(\text{Bi}) < 190$  nuclei the  $10^-$  state should not be an isomeric any more, as at least an  $8^-$  multiplet member was predicted below the  $10^-$  state. However, we note that the predicted energy difference  $8^- \rightarrow 10^-$  was only a few tens of keV and therefore the predictions [23] should be considered as indicative only. Furthermore, as explained in [1], the calculated energy splitting and relative position of the states within a given multiplet depend on the neutron occupation probabilities  $u^2$  and  $v^2$  as a function of neutron number. In particular, around a value of  $v^2(1i_{13/2}) \approx 0.6-0.7$  ( $N \approx 109-111$  in Bi nuclei, see fig. 9 and table 4 of [23]), the p-n coupling (thus, the multiplet splitting) will be turning over between particle-hole-like (for the heavier nuclei) into particle-particle-like (for the lower-mass nuclei). Therefore, depending mostly on the neutron single-particle energies and the pairing force parameters an uncertainty of about 2 mass units for the mass-dependence of the calculated results should be considered. In fact, our new data show that the  $10^-$  state is still an isomeric state in  $^{188}\text{Bi}$  [1] and, possibly, in  $^{186}\text{Bi}$ , which is in disagreement with the predictions of [23].

According to Paar's rule [24], which results in a splitting of the multiplet members as a quadratic function in spin  $J(J+1)$  (see also discussion in sect. 4.1 of [1]), the  $3^+$  state is predicted to stay lowest in the  $[\pi 1h_{9/2} \times \nu 3p_{3/2}]_{3^+ \rightarrow 6^+}$  multiplet, which was experimentally proved down to  $^{190}\text{Bi}$  [2] and in  $^{188}\text{Bi}$  [1]. As shown above, possibly, this configuration could be also responsible for the longer-lived isomer of  $^{186}\text{Bi}$ .

However, the possibility cannot be excluded that some other configurations may become important in the lightest Bi nuclei. Although the main discussion is given in sect. 4.1 of [1], for the sake of completeness we will briefly summarise the main ideas. A low-lying  $\pi 1i_{13/2}$  isomeric configuration was recently found at 252 keV in  $^{187}\text{Bi}$  [25] and at 357 keV in  $^{189}\text{Bi}$  [26, 25]. These data, combined with theoretical calculations [25], suggest that this configuration may even become the ground state in the lighter odd-mass Bi nuclei. Furthermore, for the lightest Bi and Tl isotopes beyond the neutron mid-shell at  $N = 104$  the neutron  $1i_{13/2}$  quasiparticle state will start moving up in energy and the neutron hole excitations into the  $2f_{7/2}$  or  $1h_{9/2}$  orbitals will start playing a role at low excitation energies. Finally, the oblate-prolate shape coexistence, evidence for which was recently observed in the neighbouring odd-mass Bi nuclei [27], may be also manifested in the odd-odd nuclei in this region.

Therefore, all possible proton-neutron orbital combinations leading to states with the same spin and parity should be considered while discussing the  $I^\pi$  assignments.



Clearly, more detailed experimental studies as well as calculations taking into account proton 1p regular and proton 2p-1h intruder configurations coupled to the low-lying neutron 1 quasiparticle configurations, incorporating the proton-neutron interaction explicitly as well as particle-core coupling (see ref. [23] for more details), are necessary.

### 3.2 $^{184}\text{Bi}$

By analogy with  $^{186}\text{Bi}$  we used the reduced  $\alpha$  width and  $\alpha$ -decay energy systematics to get some information on the spin/parity assignments of two isomeric states in the new isotope  $^{184}\text{Bi}$ . First of all, we note that the strongest 7194 keV and 7220 keV decays of  $^{184}\text{Bi}$  are both unhindered ( $\delta_\alpha^2(7194 \text{ keV}) = 55(10) \text{ keV}$  and  $\delta_\alpha^2(7220 \text{ keV}) = 97(30) \text{ keV}$ ), which implies that they connect states with same spin and parity in the parent and daughter nuclei. Secondly, both these energies lie close to the extrapolated values of the  $10^- \rightarrow 10^-$  and  $3^+ \rightarrow 3^+$  decays in  $^{184}\text{Bi}$  (see fig. 7a). These facts suggest that possibly the corresponding  $\alpha$ -decaying isomeric states in  $^{184}\text{Bi}$  could have the  $10^-$  and  $3^+$  assignments. However, as the extrapolation to  $^{184}\text{Bi}$  from the experimental data for  $^{188-196}\text{Bi}$  nuclei may be not reliable similarly to the case of  $^{186}\text{Bi}$  we prefer not to draw any definitive conclusions here.

### 3.3 Comparison of the $\alpha$ -decay properties of $^{184}\text{Bi}$ and $^{186}\text{Bi}$

A quite interesting fact that the energies of the strongest unhindered  $\alpha$ -decays in  $^{184}\text{Bi}$  are similar to, or even somewhat lower than those of the heavier isotope  $^{186}\text{Bi}$  (see table 1) should be underlined. Furthermore, the two isotopes have quite similar half-lives. Although no solid arguments can be given here, a possible explanation for such a behaviour could be as follows. Most probably, irrespective of exactly which configurations are involved in the  $\alpha$ -decays, the strongest (unhindered)  $\alpha$ -decay would proceed to an excited intruder configuration as is observed in the heavier isotopes  $^{188-196}\text{Bi}$ . Due to the expected increase of the excitation energy of such intruder configuration in the daughter Tl nuclei (see sect. 4.3.1 of [1] and fig. 7b of this paper), the energy of the feeding  $\alpha$ -decay will not change strongly by moving to lighter Bi isotopes, which would result in similar half-life values of neighbouring nuclei. For example, if we assumed the spin and parity of ( $10^-$ ) and ( $3^+$ ) for observed states in  $^{184,186}\text{Bi}$ , then the (nearly linear) increase of the energy of the crossover  $10^- \rightarrow 7^+$  and  $3^+ \rightarrow 2^-$   $\alpha$ -decays, when approaching  $^{184}\text{Bi}$  (see fig. 7a), would be accompanied by the expected parabolic energy increase (as a function of the neutron number) in the excitation energies of the corresponding excited intruder  $10^-$  and  $3^+$  states in the daughter Tl isotopes (see fig. 7b). Due to this the energy of the strongest unhindered  $10^- \rightarrow 10^-$  and  $3^+ \rightarrow 3^+$   $\alpha$ -decays to these intruder states would stay nearly constant or may even

become smaller compared to the heavier isotopes, which in turn would explain the longer-half-life values. This is quite a unique mechanism, which may be present only in this region.

Furthermore, the parabolic increase of the energy of the intruder states in the daughter Tl isotopes would also explain the more fragmented de-excitation path in the cases of  $^{180,182}\text{Tl}$ . We note that in [1] an intruder ( $10^-$ ) state was observed in  $^{184}\text{Tl}$  ( $N = 103$ ) at an excitation energy of 500(5) keV (see fig. 7b). Therefore, if the nearly parabolic trend (as a function of the neutron number) of the energy of the  $10^-$  intruder states in the Tl isotopes persists below  $^{184}\text{Tl}$ , then in the lighter isotopes this state will not be a long-lived isomeric state any more, as it will be able to decay to some of the lower-lying excited states. For example, in  $^{182}\text{Tl}$  the extrapolated energy of the  $10^-$  intruder state is about 680 keV (marked by a cross in fig. 7b), which should allow this state to decay to the lower-lying (unobserved)  $8^+$  state of the  $[\pi 2d_{3/2}^{-1} \times \nu 1i_{13/2}]_{5^+ \rightarrow 8^+}$  multiplet or to some other lower-lying excited configurations. We remind the reader that a few states of the  $[\pi 2d_{3/2}^{-1} \times \nu 1i_{13/2}]$  multiplet were tentatively identified in  $^{184,186}\text{Tl}$  nuclei [1]. Also, the low-lying low-spin  $2^- - 5^-$  members of the  $[\pi 1h_{9/2} \times \nu 1i_{13/2}]$  multiplet, which are predicted below the  $10^-$  state in the  $A(\text{Tl}) < 188$  nuclei [23], can be more easily populated (compared to the heavier Tl nuclei, see [1]) in the  $\alpha$ -decay of the low-spin isomer.

## 4 Conclusion

In this work we identified the new isotope  $^{184}\text{Bi}$  and presented improved data on the  $\alpha$ -decay of  $^{186}\text{Bi}$ . Similar to the heavier odd-odd mass isotopes  $^{186-192}\text{Bi}$  two  $\alpha$ -decaying isomeric states were found in  $^{184}\text{Bi}$ . Based on the  $\alpha$ - $\gamma$  coincidence measurements it was shown that the decays of  $^{184,186}\text{Bi}$  proceed via a quite complex decay path to a variety of the low-lying excited states in the respective daughter nuclei  $^{180,182}\text{Tl}$ . Most probably, the direct full energy (crossover)  $\alpha$ -decays of both isomeric states in  $^{184,186}\text{Bi}$  were not observed. The similarity of the decay energies and half-lives of  $^{184,186}\text{Bi}$  was pointed out and a possible explanation for this effect was suggested. The  $\alpha$ -branching ratio of  $^{180}\text{Tl}$  was deduced for the first time as  $b_\alpha = (2-12)\%$ .

Nevertheless, a more detailed study would be necessary in the future with a factor of at least ten higher statistics and  $\alpha$ - $\gamma$ - $\gamma$  coincidence measurements to establish the  $\alpha$ -decay schemes of both isomeric states in  $^{184,186}\text{Bi}$ . A complementary in-beam study of the excited states in the daughter isotopes  $^{180,182}\text{Tl}$  would also help to shed more light on this problem.

The importance of the GEANT simulations for the disentangling effects of the  $\alpha$ - $e^-$  energy summing in the PSSD in the experiments at the recoil separators is demonstrated.

We thank the UNILAC staff for providing the stable and high-intensity  $^{94,95}\text{Mo}$  beams. This work was supported by the Access to Large Scale Facility programme under the Training and Mobility of Researchers programme of the European Union within the contract HPRI-CT-1999-00001, by the EX-OTAG contract HPRI-1999-CT-50017, by the Interuniversity Attraction Poles Programme - Belgian State - Federal Office for Scientific, Technical and Cultural Affairs (IAP grant P5/07). K.V.d.V. is research assistant of the FWO-Vlaanderen. A.N.A. was partially supported by the GREAT contract EP-SRC GR/M79981.

## References

1. A.N. Andreyev *et al.*, this issue, p. 39.
2. P. Van Duppen *et al.*, Nucl. Phys. A **529**, 268 (1991).
3. G. Münzenberg *et al.*, Nucl. Instrum. Methods **161**, 65 (1979).
4. S. Hofmann *et al.*, Z. Phys. A **291**, 53 (1979).
5. S. Hofmann, G. Münzenberg, Rev. Mod. Phys. **72**, 733 (2000).
6. R.B. Firestone, *Table of Isotopes*, 8th edition (John Wiley and Sons, Inc., New York, 1996).
7. U.J. Schrewe *et al.*, Phys. Lett. B **91**, 46 (1980).
8. J.F.C. Cocks *et al.*, Eur. Phys. J. A **3**, 17 (1998).
9. J. Schneider, GSI report GSI-84-3, 1984, unpublished.
10. J.C. Batchelder *et al.*, Z. Phys. A **357**, 121 (1997).
11. A.N. Andreyev *et al.*, Eur. Phys. J. A **14**, 63 (2002).
12. J. Batchelder *et al.*, Eur. Phys. J. A **5**, 49 (1999).
13. J.A. Keller *et al.*, Nucl. Phys. A **452**, 173 (1986).
14. V.A. Bolshakov *et al.*, *Proceedings of the 6th International Conference on Nuclei Far From Stability and the 9th International Conference on Atomic Masses and Fundamental Constants*, IOP Conf. Proc. **132**, 743 (1993).
15. The program to calculate conversion coefficients. The National Nuclear Data Center (NNDC), <http://www.nndc.bnl.gov/nndc/physco/>.
16. A.N. Andreyev, [http://npg.dl.ac.uk/GREAT/geant\\_gr.htm](http://npg.dl.ac.uk/GREAT/geant_gr.htm); and Geant Detector Simulation Tool, CERN, 1993, <http://wwwinfo.cern.ch/asd/geant>.
17. J.O. Rasmussen, Phys. Rev. **113**, 1593 (1959).
18. C.N. Davids *et al.*, Phys. Rev. Lett. **76**, 592 (1996); G.L. Poli *et al.*, Phys. Rev. C **63**, 044304 (2001).
19. K.S. Toth *et al.*, Phys. Rev. C **58**, 1310 (1998).
20. Y.A. Akovali, Nucl. Data Sheets **84**, 1 (1998).
21. K.S. Toth *et al.*, Phys. Rev. C **60**, 011302 (1999).
22. C. Cabot *et al.*, Nucl. Phys. A **241**, 341 (1975).
23. J. Van Maldeghem, K. Heyde, Fizika **22**, 233 (1990).
24. V. Paar, Nucl. Phys. A **331**, 16 (1979).
25. A. Hürstel *et al.*, Eur. Phys. J. A **15**, 329 (2002).
26. A.N. Andreyev *et al.*, Eur. Phys. J. A **10**, 129 (2001).
27. A. Hürstel, private communication (2002).